

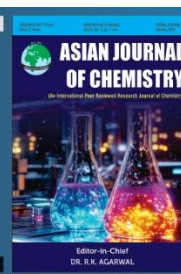


Asian Journal of Chemistry;

Vol. 37, No. 9 (2025), 2155-2158

ASIAN JOURNAL OF CHEMISTRY

<https://doi.org/10.14233/ajchem.2025.32841>



Synthesis, Characterization of Transition Metal (Mn, V) based Silvertone Type Anion and its Antioxidant and Antimicrobial Studies

ALPHONSE LAZAR[✉], RAJESH KUMAR[✉], VICKRAM MANI, BHARATH SAMANNAN[✉] and JEYABALAN THAVASIKANI*

Department of Chemistry, Sacred Heart College (Autonomous) (Affiliated to Thiruvalluvar University, Vellore), Tirupattur-635601, India

*Corresponding author: E-mail: jayabalandr@gmail.com

Received: 5 October 2024

Accepted: 19 July 2025

Published online: 30 August 2025

AJC-22094

Transition metals (Mn, V) based oxo-anions (hybrid materials) were synthesized and characterized by X-ray powder diffraction, UV-visible and infrared spectral analysis. Metal-based polyoxo anion (POM) hybrid materials reflect stronger antioxidant potential as indicated by their higher DPPH scavenging activity. The synthesized POM compounds also exhibit enhanced bacterial activity of 21 ± 2 and 17 ± 3 $\mu\text{g/mL}$ against *Staphylococcus aureus* (Gram-positive) and *Escherichia coli* (Gram-negative), respectively. The efficacy of the synthesized hybrid materials can be attributed to the synergistic effects of the cations and oxo-anions, which lead to more potent derivatives with a broader spectrum of antibacterial activity.

Keywords: Hybrid materials, Polyoxo anions, Transition metals, Biological studies.

INTRODUCTION

Hybrid materials consist of two or more distinct components that are combined to form a new material with unique properties. The components can be of different chemical compositions or phases. The term polyoxometalate (POM) is applied to a large group of generally anionic clusters with frameworks built from transition metal oxo anions linked by shared oxide ions [1]. They exhibit a wide range of structural and chemical properties, making them useful in a variety of applications such as catalysis, energy storage and material science [2-6].

Hybrid materials are based on transition metal oxo-clusters. This is a new class of advanced materials that have attracted significant attention in recent years due to their unique properties and potential applications [7]. Transition metal oxoclusters are clusters of transition metal atoms that are bound together by oxygen atoms. POMs are of high diversity of composition, size and structure. Depending on their compositions, they can be classified into two categories *e.g.* isopolyoxometalates consisting only one set of polyanions $[\text{M}_m\text{O}_y]^{p-}$ and hetero-polyoxometalates consisting more than one set of polyanions $[\text{X}_x\text{M}_m\text{O}_y]^{p-}$ where X atom refers to Mn and V [8]. The metal element M, usually in an octahedral, tetrahedral or rarely trigonal bipyramidal environment of

oxygen atoms. Cluster gives rise to existence of a large number of rigid and stable structural isomers.

Furthermore, isomerization has already been identified theoretically and experimentally in the classical Keggin, Dawson, Anderson, Lindqvist-type phases and many other clusters [9]. The synthesis of POMs and their antibacterial activity can depend on the choice of metal ions, the type of ligands and the overall structure of the molecule [10]. Manganese and vanadium substituted POMs (Mn-POMs, V-POMs) become visible to attract the significant attention due to their variable oxidation states, redox properties, magnetic properties and other chemical properties [11,12]. It has been considered as unique metal center and plays crucial role in many catalytic pathway, magnetism and biological activity.

EXPERIMENTAL

All chemicals and reagents were purchased from Merck, USA and used as such. IR spectra were recorded in the range $4000\text{--}400\text{ cm}^{-1}$ on an Alpha Centaur FT/IR spectrophotometer using KBr pellets. Diffused reflectance UV-Vis absorption spectra were obtained using Shimadzu ISR-3100 UV-Vis-NIR scanning spectrophotometer in range of $200\text{--}800\text{ nm}$. PXRD patterns were recorded using Bruker D2 phaser (source $\text{CuK}\alpha$ radiation, $\lambda = 1.5418\text{ \AA}$) in the range $0\text{--}90^\circ$.

This is an open access journal, and articles are distributed under the terms of the Attribution 4.0 International (CC BY 4.0) License. This license lets others distribute, remix, tweak, and build upon your work, even commercially, as long as they credit the author for the original creation. You must give appropriate credit, provide a link to the license, and indicate if changes were made.

Synthesis of transition metal-based silvertone-type anion (STA) complexes

Vanadium based STA: To synthesize vanadium-based silvertone-type anion (STA), ammonium ceric sulphate (0 mmol) and ammonium heptamolybdate (0.5 mmol) were dissolved in 30 mL of H₂O separately and mixed well under constant stirring [13]. To this solution, vanadyl sulphate (0.5 mmol) dissolved in 15 mL water was then added and stirred for 10-15 min in the presence of few drops of conc. HNO₃. The solution was continuously stirred for another 1.5-2 h. A green colour precipitate was obtained and filtered and dried at room temperature.

Manganese based STA: The manganese-based silvertone-type anion (STA) was synthesized following a procedure similar to the above method, except that 0.5 mmol of manganese(II) sulfate was separately dissolved in 15 mL of water. A small quantity of potassium persulfate was subsequently added to promote the oxidation of manganese. This solution was stirred for 10-15 min in the presence of a few drops of conc. HNO₃ and continued for another 1.5-2 h. A pale yellow colour precipitate was obtained and filtered then dried at room temperature.

Antioxidant assay: The antioxidant activity of the synthesized transition metal based (Mn, V) oxo-anions (hybrid materials) was evaluated by DPPH assay with slight alterations in 96-microwell plates [14]. The working concentrations for the hybrid materials and reference ascorbic acid ranged from 250 to 16,000 µg/mL in DMSO solvent. To evaluate the antioxidant activity, 100 µL of a 100 mM DPPH solution was added to the sample suspensions and incubated in dark at room temperature for 0.5 h. Absorbance was measured at 517 nm over 2 h using a multiwell plate reader and DMSO was used as blank. The IC₅₀ is defined as the concentration required to reduce the initial DPPH absorbance by 50% was determined as the average of three replicates.

Antimicrobial activity: To investigate the antimicrobial resistance, *Staphylococcus aureus* and *Escherichia coli* were selected as model Gram-positive and Gram-negative pathogens, respectively, in this study [15]. The material was placed over a ciprofloxacin disk to evaluate its effect on antimicrobial resistance using the disk diffusion method under ionized and metallized conditions. The bacteria were cultured overnight in a flask accommodated by liquid Luria-Bertani (LB, 25 g/L) under incubator shaker at 37 °C. At the same time, 25 g/L fresh LB agar with the curing agent (agar, 15 g/L) was poured in a petridish, while solidifying at room temperature [16]. Afterwards, the cultured *S. aureus* and *E. coli* mixture (200 mL) was extended evenly on the solidified LB agar plates. Subsequently, the polyoxometalate complexes were sterilized under ultraviolet (UV) radiation for 30 min while placed on the surface of LB agar in Petri dishes. The inoculated plates were then incubated at room temperature overnight to allow bacterial growth. Zones of inhibition around the disks were recorded [9,17].

RESULTS AND DISCUSSION

FT-IR: FT-IR spectra of silvertone-type anion transition metal-based STA are shown in Fig. 1. The finger print region of STA is present between 1200-450 cm⁻¹ [18]. The STA clearly shows the four key peaks of (M-O_t) terminal oxygen bridging, (M-O_b) intra/inter-oxygen bridging, M-O-M and M-O (M = V, Mn) which are attributed to 1184 cm⁻¹ and 1094 cm⁻¹, 939 and 896 cm⁻¹, 843 cm⁻¹ and 521 cm⁻¹ [19]. The peak at 475 cm⁻¹ corresponds to Mn-O bond [20]. The IR spectral data of metal doped STA are given in Table-1.

UV-visible spectroscopy: The Mn-STA material exhibits absorption bands at 232 nm and 201 nm (Fig. 2a), which correspond to STA, with a calculated band gap of 5.34 eV [21]. In comparison, the V-STA complex shows the absorp-

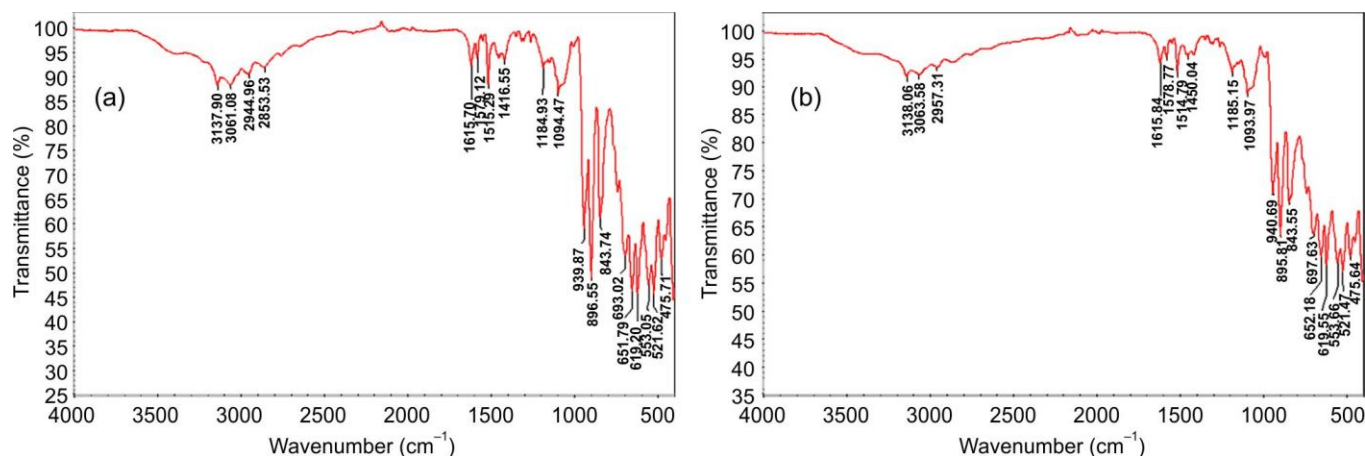


Fig. 1. FT-IR spectra of (a) Mn-STA and (b) V-STA

TABLE-1
FT-IR SPECTRAL DATA OF Mn-STA AND V-STA

Compounds	Vibrational frequencies (cm ⁻¹)					
	-OH	M-O	M-O _t	M-O _b	M-O-M	M-O (M = V, Mn)
Mn-STA	3061	475	1184, 1094	939, 896	843	521
V-STA	3063	475	1185, 1093	940, 895	843	521

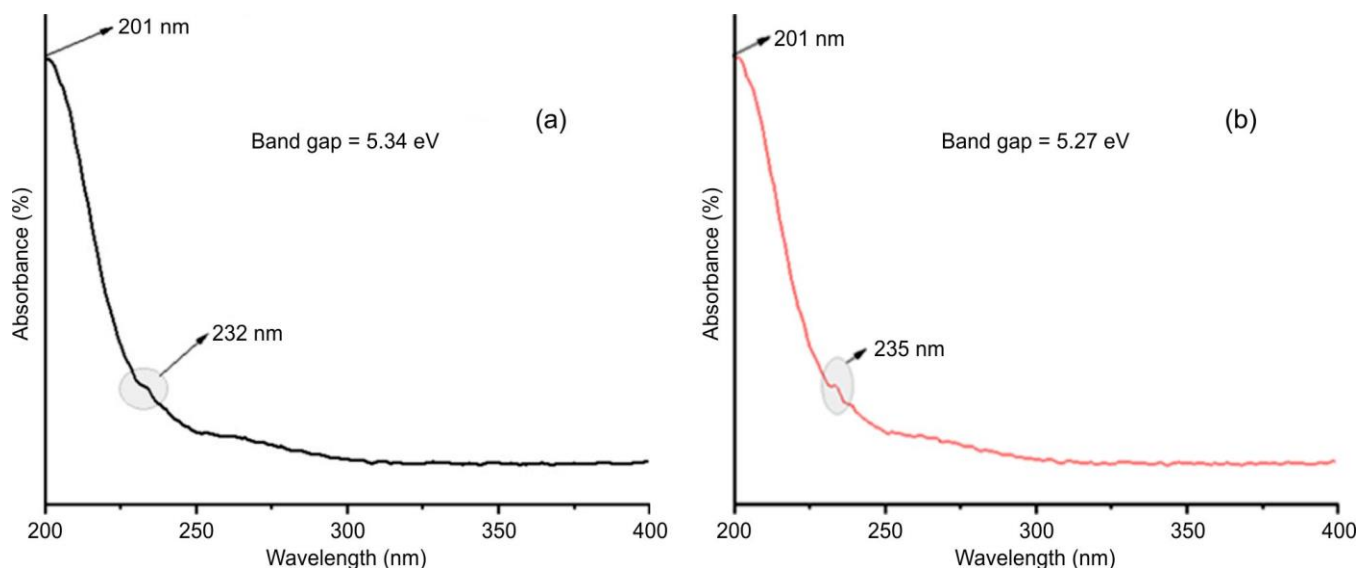


Fig. 2. UV-Vis spectra of (a) Mn-STA and (b) V-STA

tion bands at 201 nm and 235 nm (Fig. 2b), indicating a significant blue shift. The corresponding band gap for V-STA was found to be 5.27 eV. Since, the absorption bands of both Mn-STA and V-STA appear in the region between 232-235 nm, which are due to ligand-metal charge transfer (LMCT) or oxygen to metal charge transfer (OMCT).

X-Ray diffraction (XRD) studies: The peaks at 9.85° , 10.52° , 11.81° , 21.39° , 25.46° , 26.41° , 28.71° , 30.00° , 45.15° and 57.50° correspond to 12-B polyacids where Mn is present in the Mn-STA hybrid material (Fig. 3a). Whereas in V-STA hybrid material, the XRD peaks at 9.85° , 10.66° , 11.87° , 21.39° , 25.60° , 26.41° , 28.86° , 36.87° , 45.42° and 57.50° also correspond to 12-B polyacid [22,23].

Antioxidant activity: The antioxidant potential of the hybrid materials (V-STA and Mn-STA) was determined using the DPPH assay. As observed in Table-2, the antioxidant activity increases with concentration of the compounds. Ascorbic acid exhibits the highest radical scavenging activity, reaching 70.12 mg/100 g at the highest concentration of 100

Conc. ($\mu\text{g/mL}$)	Ascorbic acid	V-STA	Mn-STA
20	17.44	14.1	13.25
40	30.23	28.28	30.13
60	43.77	35.15	47.89
80	55.43	52.17	58.35
100	70.12	68.26	69.81

mg/mL. Both the hybrid materials, V-STA and Mn-STA follow a similar trend but show slightly lower values of 68.26 and 69.81 mg/100 g, respectively, at the same concentration. The IC_{50} value for the standard ascorbic acid was found to be 50 mg/mL, while the IC_{50} values for STA-V and STA-Mn would be lower, reflecting stronger antioxidant potential as indicated by their higher DPPH scavenging activity at each concentration. Based on the data, both the hybrid materials demonstrate strong antioxidant properties and could be explored further as potential natural antioxidants for various applications.

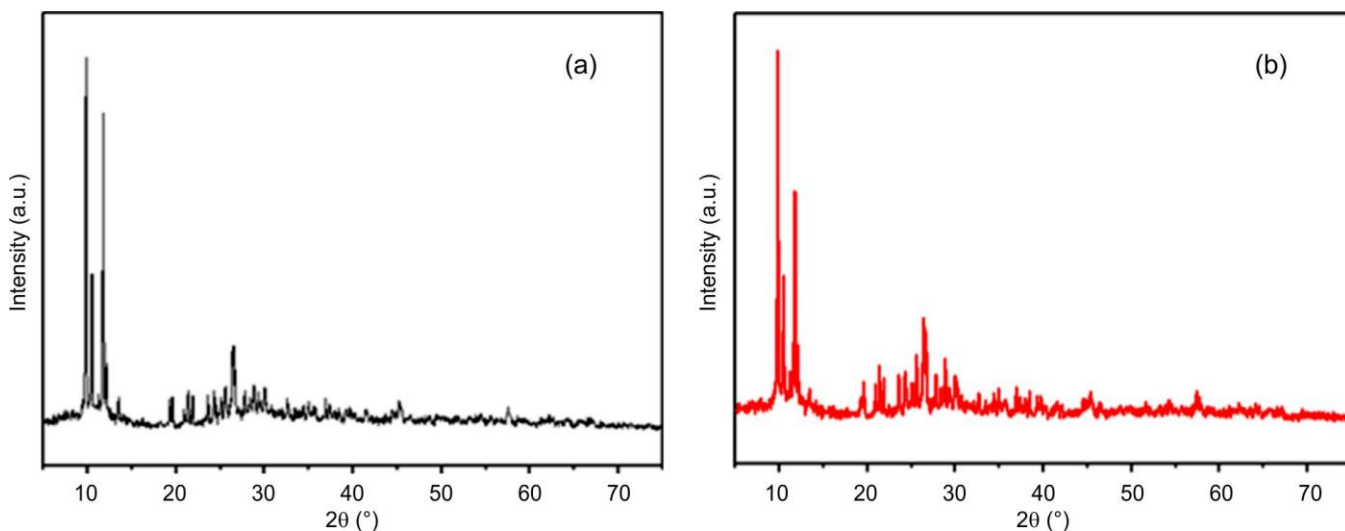


Fig. 3. XRD patterns of (a) Mn-STA and (b) V-STA

Antimicrobial activity: The results showed that the Mn-STA material has higher antibacterial activity against *S. aureus* and *E. coli*, with an inhibition zone of 21 ± 1 mm and 20 ± 2 mm, respectively. This suggests that the Mn-STA material exhibits broad-spectrum of antimicrobial properties, inhibiting both Gram-positive and Gram-negative bacteria effectively. The V-STA exhibits comparable antibacterial effect, producing inhibition zones of 20 ± 2 mm for *S. aureus* and 20 ± 3 mm for *E. coli*. This indicates that the vanadium hybrid material also possesses broad-spectrum of antimicrobial activity. The antimicrobial performance of these compounds could be attributed to the presence of metal ions, which are known to disrupt bacterial cell walls and interfere with intracellular processes [24,25].

Conclusion

Two new polyoxometalates *i.e.* M-STA (where M = Mn, V and STA is the silvertion-type anion) were synthesized and characterized using spectroscopic techniques such as FT-IR UV and X-ray diffraction (XRD). Both polyoxometalates STA-V and STA-Mn reflect stronger antioxidant potential as indicated by their higher DPPH scavenging activity at different concentrations. The antimicrobial activity were also carried out for the polyoxometalates complexes and showed the enhanced antibacterial activity against the studied pathogens.

ACKNOWLEDGEMENTS

This work was fully supported by the Management of Sacred Heart College (Autonomous), Tirupattur District, Tamil Nadu, India, through Don Bosco Research Grant (Ref: SHC/DB Grant/2024/06). We would like to express our in-depth gratitude to the Secretary and Principal of Sacred Heart College, Tirupattur.

CONFLICT OF INTEREST

The authors declare that there is no conflict of interests regarding the publication of this article.

REFERENCES

1. B. Samannan and J. Thavasikani, *Inorg. Chem. Commun.*, **170**, 113162 (2024); <https://doi.org/10.1016/j.inoche.2024.113162>
2. K. Yonesato, D. Yanai, K. Yamaguchi and K. Suzuki, *Chem. Eur. J.*, **31**, e202500877 (2025); <https://doi.org/10.1002/chem.202500877>
3. K. Li, T. Liu, J. Ying, A. Tian and X. Wang, *J. Mater. Chem. A*, **12**, 13576 (2024); <https://doi.org/10.1039/D4TA01636J>
4. Y. Zhang, Y. Li, H. Guo, Y. Guob and R. Song, *Mater. Chem. Front.*, **8**, 732 (2024); <https://doi.org/10.1039/D3QM01000G>
5. M. Moghadasi, M. Abbasi, M. Mousavi and M. Mirzaei, *Dalton Trans.*, **54**, 6333 (2025); <https://doi.org/10.1039/D4DT03428G>
6. B. Samannan, P. Peter and J. Thavasikani, *J. Appl. Surf. Sci. Adv.*, **100**, 359 (2023).
7. S. Bharath, A. Lazer, Y.-L. Lin, P. Peter and J. Thavasikani, *Spectrochim. Acta A Mol. Biomol. Spectrosc.*, **299**, 122868 (2023); <https://doi.org/10.1016/j.saa.2023.122868>
8. R. Murugesan, P. Sami, T. Jeyabalan and A. Shunmugasundaram, *Transition Met. Chem.*, **23**, 583 (1998); <https://doi.org/10.1023/A:1006972301876>
9. M.T. Pope, M. Sadakane and U. Kortz, *Eur. J. Inorg. Chem.*, **2019**, 340 (2019); <https://doi.org/10.1002/ejic.201801543>
10. B. Samannan, J. Selvam, Y.-L. Lin, P. Peter and J. Thavasikani, *Turk. J. Chem.*, **47**, 364 (2023); <https://doi.org/10.55730/1300-0527.3543>
11. R. Murugesan, T. Jeyabalan and P. Sami., *Proc. Indian. Acad. Sci.*, **110**, 7 (1998); <https://doi.org/10.1007/BF02871905>
12. M.R. Horn, A. Singh, S. Alomari, S. Goberna-Ferrón, R. Benages-Vilau, N. Chodankar, N. Motta, K. Ostrikov, J. MacLeod, P. Sonar, P. Gomez-Romero and D. Dubal, *Energy Environ. Sci.*, **14**, 1652 (2021); <https://doi.org/10.1039/D0EE03407J>
13. N.I. Gumerova and A. Rompel, *Inorg. Chem.*, **60**, 6109 (2021); <https://doi.org/10.1021/acs.inorgchem.1c00125>
14. L. Yao, Z. Long, Z. Chen, Q. Cheng, Y. Liao and M. Tian, *Membranes*, **10**, 214 (2020); <https://doi.org/10.3390/membranes10090214>
15. M. Zhang, X. Xin, Y. Feng, J. Zhang, H. Lv and G.-Y. Yang, *Appl. Catal. B*, **303**, 120893 (2022); <https://doi.org/10.1016/j.apcatb.2021.120893>
16. C. Streb, K. Kastner and J. Tucher, *Phys. Sci. Rev.*, **4**, 20170177 (2019); <https://doi.org/10.1515/psr-2017-0177>
17. P.-E. Car and G.R. Patzke, *Inorganics*, **3**, 511 (2015); <https://doi.org/10.3390/inorganics3040511>
18. S. Lis, *J. Alloys Compd.*, **300–301**, 88 (2000); [https://doi.org/10.1016/S0925-8388\(99\)00736-7](https://doi.org/10.1016/S0925-8388(99)00736-7)
19. M. Xu, C. Liu, Y. Wang, J. Wang, J. Feng, and J. Sha, *J. Clust. Sci.*, **32**, 1543 (2021); <https://doi.org/10.1007/s10876-020-01845-0>
20. T. Jeyabalan, P. Sami, A. Shunmugasundaram and R. Murugesan, *Spectrochim. Acta A Mol. Biomol. Spectrosc.*, **55**, 2187 (1999); [https://doi.org/10.1016/S1386-1425\(99\)00015-3](https://doi.org/10.1016/S1386-1425(99)00015-3)
21. T. Quanten, P. Shestakova, D. Van Den Bulck, C. Kirschhock and T.N. Parac-Vogt, *Chem. Eur. J.*, **22**, 3775 (2016); <https://doi.org/10.1002/chem.201503976>
22. M.R. Horn, A. Singh, S. Alomari, S. Goberna-Ferron, R. Benages-Vilau, N. Chodankar, N. Motta, K.K. Ostrikov, J. MacLeod, P. Sonar, P. Gomez-Romero and D. Dubal, *Energy Environ. Sci.*, **14**, 1652 (2021); <https://doi.org/10.1039/D0EE03407J>
23. J.-C. Liu, J.-W. Zhao, C. Streb and Y.-F. Song, *Coord. Chem. Rev.*, **471**, 214734 (2022); <https://doi.org/10.1016/j.ccr.2022.214734>
24. Z. Liang, H. Cheng and Q. Mao, *J. Mol. Liq.*, **121**, 483 (2023).
25. M. Jamie Cameron, Sharad S.A, Guillaume Izzet, *Chem. Soc. Rev.*, **•••**, 293 (2022).